

**DROPLET TURBULENCE INTERACTIONS
UNDER SUBCRITICAL AND SUPERCRITICAL CONDITIONS**

E. B. Coy, S. C. Greenfield, M. S. Ondas,
Y. -H. Song, T. D. Spegar, and D. A. Santavicca
Penn State University

The goal of this research is to experimentally characterize the behavior of droplets in vaporizing liquid sprays under conditions typical of those encountered in high pressure combustion systems such as liquid fueled rocket engines. Of particular interest are measurements of droplet drag, droplet heating, droplet vaporization, droplet distortion, and secondary droplet breakup, under both subcritical and supercritical conditions. The following is a brief description of the specific accomplishments which have been made over this past year.

Measurements of the Dynamics of Droplet-Turbulence Interactions (E.B. Coy)

Preliminary experiments have been performed on the motion of droplets in the self-generated turbulence of a spray. The following results demonstrate the capability of the measurement technique for determining the size-velocity correlation.

Experimental Apparatus: A schematic drawing of the apparatus is shown in Figure 1. It is basically an adaptation of the Particle Image Velocimetry technique.¹ The laser beams are focused into sheets which coincide with the image plane of the 35mm camera. The camera shutter is opened and the lasers are fired in rapid succession forming two distinct images of each droplet. The components of droplet velocity in the object plane are determined from the displacement of the images and the time interval between pulses. Matching the droplet images is facilitated if the order of laser pulses can be distinguished by color. This is accomplished by doping the liquid with two fluorescent dyes (e.g., Rhodamine 610 and Stilbene 420). Rhodamine 610 absorbs at the second harmonic (532 nm) and emits at 610 nm while Stilbene 420 absorbs at the third harmonic (355 nm) and emits at 420 nm. These characteristics permit the intense elastic scattering of the excitation wavelengths to be eliminated with a narrow band mirror and edge filter thus permitting only the fluorescent emission from the droplets to be captured on 35 mm color slide film. The images are recorded at 2:1 magnification which gives a field of view of 18 mm by 12 mm. The film used is ASA 200 color reversal film (e.g., Kodak Ektachrome 200).

The slides are automatically analyzed using a microcomputer based image processing system. The slides are placed in a translation stage system which positions the slide relative to an RS-170, CCD camera and allows the slide to be analyzed in 225 fields, 2.4 mm wide by 1.6 mm high. For each field an image of the blue droplets is obtained by interposing a bandpass filter between the quartz-halogen lamp and the slide. The digitized image is scanned and the droplets are located and sized. The process is repeated for the red droplets.

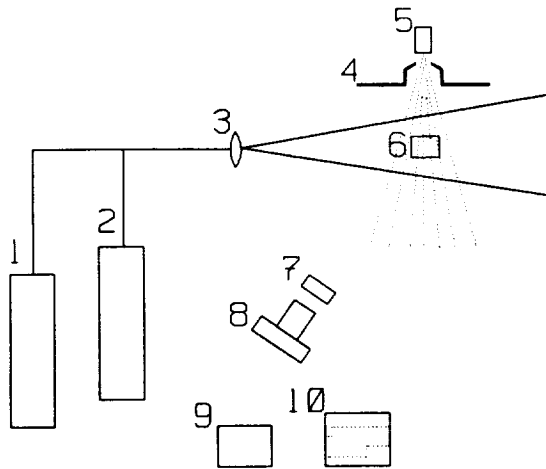


Figure 1. Experimental Apparatus: 1-355nm beam, 2-532nm beam, 3-light sheet optics, 4-skimmer, 5-nozzle, 6-sample volume, 7-532nm mirror, 8-35mm camera, 9-timing circuit, 10-oscilloscope

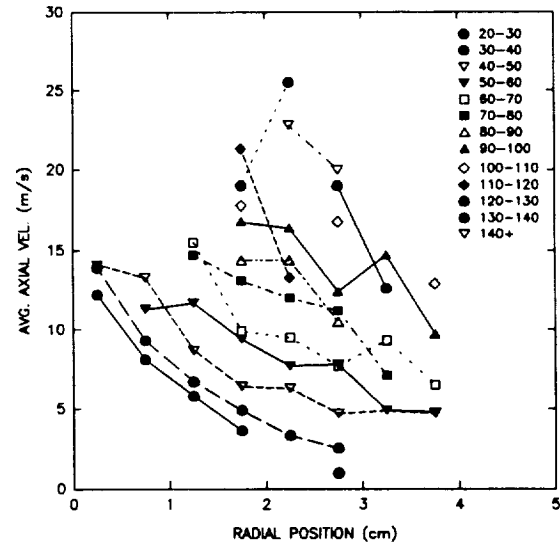


Figure 2. Average velocity as function of radial position for several size ranges of droplets for WDB 4.0 atomizer

The drop size and position is stored for post processing for velocity. The time required to analyze a single slide containing about 1000 droplet images is about 25 minutes.

Size-Velocity Data: Droplet image velocimetry measurements were made along a radius 5 cm below the nozzle exit for three nozzles. Average axial velocity as a function of radial position for several drop sizes is shown in Figure 2. It appears that larger samples will be required to achieve smooth velocity profiles; however, the trends with respect to drop size and radial position are evident and the velocities of the largest droplets agree favorably with the initial axial velocity based on thrust and mass flow. The large droplets are clustered about the 2 cm radial position indicating that the initial direction acquired at the breakup of the cone has not been significantly modified by the gas flow. The large droplets also are traveling at velocities approaching the outlet velocity. Small droplet velocities have already assumed the characteristic Gaussian profile of a turbulent jet.

An Experimental Study of Droplet Motion in Laminar and Highly Turbulent Flows (Y.-H. Song)

Overview: The objective of this study is to experimentally study the motion of droplets undergoing unsteady curvilinear motion in laminar and turbulent flows. Droplet or particle motion has been studied for a long time, and some aspects of droplet motion are well understood. For example, for a non-vaporizing solid sphere undergoing steady rectilinear motion in a laminar flow, the standard drag curve and the steady equation of motion can be used to accurately predict the sphere's velocity and trajectory. However, for the case of droplet motion in actual spray combustion systems, where vaporization, unsteady curvilinear motion and free-stream turbulence must also be accounted for, such information is not available. In order to study these effects on droplet motion, small (90-300 μm) single droplets were transversely injected into an air flow, producing

unsteady curvilinear trajectories. The present experiments were conducted using the experimental apparatus shown schematically in Figure 3, which has the capability of generating laminar or highly turbulent flows (up to 40% relative turbulence intensity) with variable temperature (up to 700 K) and pressure (up to 70 atm) conditions. The droplet Reynolds numbers investigated in this study range from 10 to 500, which covers typical droplet Reynolds numbers in spray combustion systems.

Results: Presented below are results on the effect of vaporization on droplet drag in a laminar flow and the increased droplet drag forces in a turbulent flow. The experimentally obtained drag coefficients in a laminar flow, without and with correcting for vaporization, are compared with the standard drag correlation in Figures 4-a and 4-b, respectively. In Figure 4-a, the droplet Reynolds numbers are calculated using the free stream air density and viscosity. In Figure 4-b, the droplet Reynolds numbers are estimated using the 1/3 rule, and the measured drag coefficients are multiplied by $(1+B)^{0.32}$ to correct for vaporization. Figure 4-a shows that the drag coefficients of evaporating droplets are significantly reduced as the air temperature increases. As shown in Figure 4-b, if the effect of vaporization on drag is included, the measured drag coefficients agree well with the standard drag curve.

Measured droplet acceleration in a turbulent flow is compared with the estimated droplet acceleration using the standard drag curve in Figure 5. These results show that the time averaged drag force ($m \cdot a$) in a turbulent flow is larger than that in a laminar flow at the same droplet Reynolds number, which indicates that free-stream turbulence increases the momentum transfer rate (drag force).

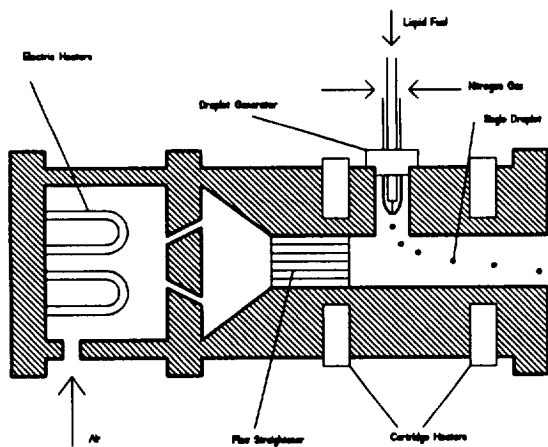


Figure 3. Schematic of Experimental Apparatus

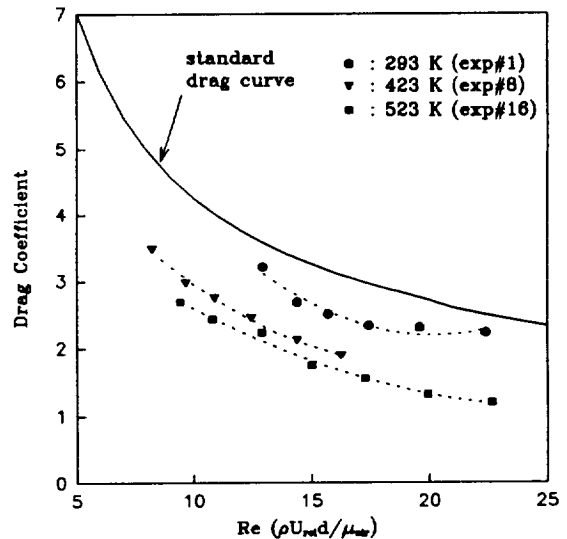


Figure 4-a. Measured drag coefficients at different temperatures

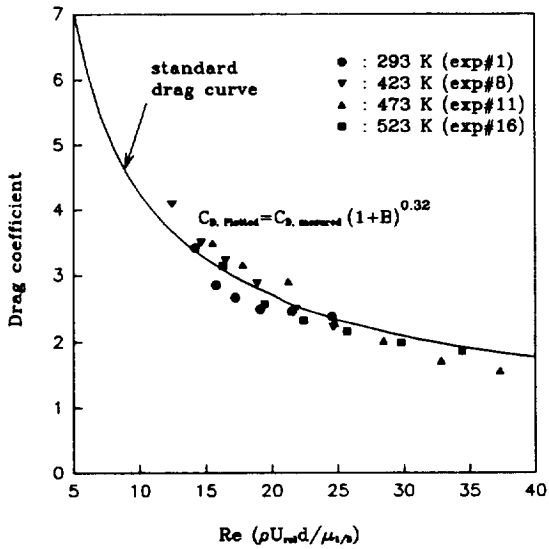


Figure 4-b. Corrected drag coefficients at different temperatures

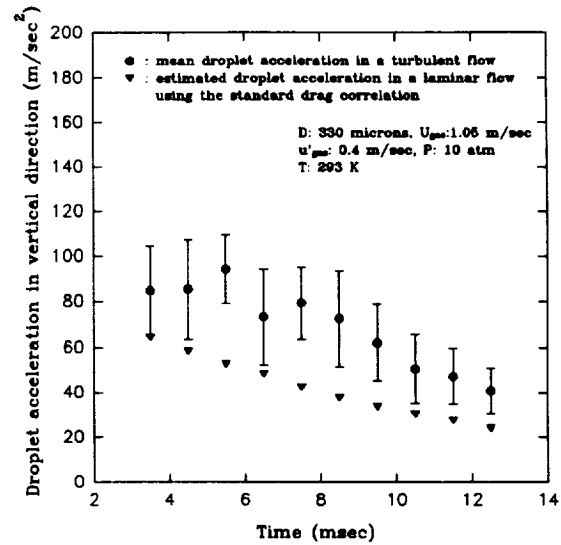


Figure 5. Measured and estimated droplet acceleration in a turbulent flow

Exciplex Thermometry (S.C. Greenfield)

Measurement of droplet temperature is important because of its influence on droplet vaporization, e.g., droplet models require droplet temperatures to accurately predict vaporization rates. Most prior experiments involved the suspension of a droplet on a thermocouple, however, this disrupts both the internal and external flowfields of the droplet. Exciplex thermometry has the advantage of being a non-intrusive fluorescence technique, thus preserving the natural flowfields surrounding and within the droplet.

The exciplex system chosen for this experiment was 2.5% (by weight) tetramethyl-1,4-phenylenediamine (TMPD) and 1.0% 1-methylnaphthalene (1MN) in tetradecane (TD). Upon UV-laser excitation (Nd:YAG, 355 nm), two distinct fluorescence signals are produced, centered at 400 nm and 500 nm. The ratio of intensities at these two wavelengths is temperature-dependent and upon calibration, can be used as a thermometer. These chemicals were chosen for both their exciplex-forming capabilities and because their boiling points are similar (TMPD-260°C, 1MN-242°C, TD-252°C). This is important because the intensity ratio versus temperature curve is concentration-dependent; differential component vaporization would bias the measurements, especially at elevated temperatures.

Many attempts were made to produce a calibration curve using droplets of known temperature. Unfortunately, wide variability existed in the intensity ratio measurements of droplets presumably at the same temperature. Three of the most probable causes of this variability can be identified. First, even though the droplets were preheated for isothermal injection into the surrounding environment, vaporization would still cool the droplets; thus, the exact temperature was uncertain. Second, the purchased TMPD showed a fairly high degree of oxidation, the affect of which is not yet fully known. Finally, there appears to be a viewing angle affect resulting from the use of a split-image filter (which produces two images of one object) to simultaneously

image the exciplex (500 nm) and monomer (400 nm) fluorescence. Because a droplet is three-dimensional and not planar, the two images appear to emanate from different parts of the droplet, the left image biased towards the front of the droplet and the right towards the back. Thus, as the droplet location changes from left to right, the region that is imaged changes as well. Since the fluorescence is more intense on the front face (i.e., in the optically thick case, where the laser first contacts the droplet), the intensity ratio will be biased by the droplet location within the field of view.

To circumvent these problems, a new experiment was designed. Instead of droplets, an Amersil TO8 quartz tube (1 mm ID, 2 mm OD) containing a thermocouple was used for calibration purposes. A 120 micron pinhole was placed in front of the tubing to prevent image overlap (caused by the split-image filter) during acquisition. Additionally, a sublimation unit was purchased to purify the TMPD. An initial set of calibration data was acquired with a Princeton Instruments intensified CCD camera and is shown in Figure 6.

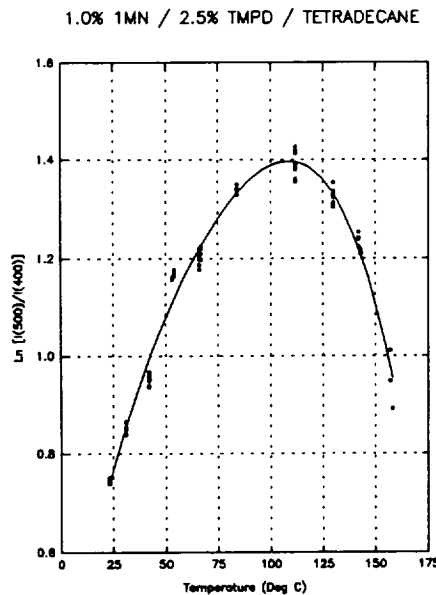


Figure 6. Exciplex Calibration Curve

Droplet Vaporization in an Acoustic Field (M.S. Onda)

In recent years, there has been much discussion about what mechanisms may be responsible for high frequency combustion instabilities. Some reasons for this discussion are the destructive nature of high frequency instabilities and the current lack of fundamental knowledge about their causes and sustaining mechanisms. During the JANNAF sponsored workshop on Liquid Rocket Engine Combustion Driven Instability Mechanisms,² five categories of basic combustion physics were identified: fluid mechanics, injection,

atomization, vaporization, and mixing. These mechanisms were discussed and then ranked according to how important each is likely to be to the instability process. Vaporization was considered to be a priority issue in both the subcritical and supercritical regimes. Fundamental data on the vaporization process is critical for basic physical understanding as well as for providing a database for analytical and computational models.

In order to obtain information on vaporization rates and vapor concentration wake structure around the droplet, a single vaporizing droplet is used. This is done to eliminate any possible coupling effects with other mechanisms, such as atomization. A droplet is either suspended from the end of a syringe or transversely injected into a 1.9 cm square duct with a length of 259 cm. The mean velocity of the flow is up to 10 m/s with an average pressure of up to 10.0 atm and temperature capabilities of up to 260°C. A six-orifice rotating disk is used to periodically open and close the end of the duct. With this technique, standing longitudinal waves from 100 to 500 Hz can be generated with peak to peak amplitudes of up to $\pm 10\%$ of the mean chamber pressure.

The most recent work was done using two different visualization techniques. The first technique was an exciplex vapor/liquid visualization system. Tetradecane was doped with the exciplex additives and the vaporizing droplets were suspended by a syringe tip and illuminated using either the 355 nm or the 266 nm beam from an Nd:YAG laser. The flow conditions were 1.3 m/s at 220°C and a pressure of 7.8 atm. The filtered image showing the vapor wake signal was recorded using a Princeton Instruments intensified CCD array camera. This technique provided some images of the vapor wake, but the signal to noise ratio was low. In order to increase the amount of fuel vapor in the wake, a more volatile fuel was used. The second technique used acetone as the fuel. Acetone is very volatile and it also fluoresces when excited by an ultraviolet laser source. The flow conditions were from 1.2-1.5 m/s at 50-85°C and 6.4 atm. The 266 nm beam from an Nd:YAG laser was used as the excitation source. The images were once again obtained using the intensified array camera. Due to the increased volatility of the acetone, the image quality was better than those obtained with the tetradecane exciplex mixture.

One problem that remains is the effect the syringe has on the droplet. The droplet tends to adhere to the syringe and form a teardrop shape. This is undesirable since the droplets are no longer spherical and because of the disruption in the flow field around the droplet. Also, the syringe causes some scattering of the incident laser sheet. The upcoming experiments will use an acetone droplet that is in free fall to alleviate the interference from the syringe. The droplet and its vapor wake will be illuminated by a laser sheet cutting the vertical plane of motion. The CCD array camera will be focused on this plane to record the image. Once the data acquisition system is more fully developed and images are of sufficient quality, an acoustic field will be induced on the mean gas flow and droplet vaporization in the presence of an acoustic wave can be studied.

Raman Imaging of Supercritical Droplets and Jets (T. D. Spegar)

In liquid propellant rocket engines, the behavior of the injected liquid highly influences the subsequent combustion process. Often, the combustion chamber pressure and temperature exceed the critical temperature

and pressure of the injected fuel and/or oxidizer. Transport processes in the spray dictate how the temperature of the droplets will change. Since the temperature of the combustion chamber generally surpasses the liquid temperature at injection, one might expect the liquid temperature to increase and approach the surrounding temperature. However, conditions may exist where the vaporization rate is so high that the droplet temperature decreases or total vaporization is achieved before the droplet reaches its critical temperature. But, if the droplet temperature approaches or exceeds its critical temperature, the corresponding decrease in surface tension will play an important role in droplet behavior. Specifically, droplet distortion, breakup, vaporization rate and drag, as well as enhanced permeation of the surrounding gas, can be significantly affected by a decrease or absence of surface tension. The objective of this work is to experimentally investigate the above phenomena in the helium-nitrogen system. Helium and nitrogen have highly dissimilar critical temperatures and pressures, much as the hydrogen-oxygen system.

Liquid nitrogen is injected into a helium environment at pressures up to 100 atmospheres. The injection was previously collinear with a downward helium flow but the problem of helium cooling from the droplet generator was encountered. Being cooler, the helium disturbed the field of view below the injection point due to the presence of density fluctuations. The test chamber has since been mounted on its side, with nitrogen injection downward into a crossflow of helium which can be adjusted to continuously flush the field of view. The helium velocity may also be increased to observe the effect of a strong crossflow on jet and droplet behavior. Pressurized liquid nitrogen is obtained by condensing high-pressure gaseous nitrogen upstream of the jet within the liquid nitrogen-cooled droplet generator. Jet velocity can now be measured indirectly by use of a small pressurized rotameter in the nitrogen supply line. The jet diameter is 0.004" which produces droplets of about 100 microns in diameter.

Single droplets and jets of liquid nitrogen have been injected into the helium environment at selected pressures and were viewed using a CCD video camera. Various jet structures have been observed to occur at different experimental conditions. In particular, pressure appears to play an important role in jet behavior. Using a flashlamp-pumped dye laser and an intensified CCD camera, Raman scattering measurements have been initiated to determine relative nitrogen concentrations in the jet and droplet wakes and possibly within the jet and droplets themselves. The latter technique is much more difficult due to the intense elastic scattering off the liquid surface, but may be accomplished if the liquid reaches its supercritical temperature causing the surface to no longer be well defined.

References

1. Adrian, R.J., Multi-point Optical Measurements of Simultaneous Vectors in Unsteady Flow - A Review, *Int. J. Heat and Fluid Flow*, 1986.
2. Jensen, R.J., "A Summary of the JANNAF Workshop on Liquid Rocket Engine Combustion Driven Instability Mechanisms", presented at the 26th JANNAF Combustion Meeting, Pasadena, CA, October, 1989.